



ORIGINAL ARTICLE

An MHD Casson fluid flow past a porous stretching sheet with threshold Non-Fourier heat flux model



A.B. Vishalakshi ^a, U.S. Mahabaleshwar ^{a,*}, M.H. Ahmadi ^{b,*}, Mohsen Sharifpur ^{c,d,*}

^a Department of Mathematics, Shivagangotri, Davangere University, Davangere, India

^b Department of Mechanical Engineering, Shahrood University of Technology, Iran

^c Department of Mechanical and Aeronautical Engineering, University of Pretoria, Pretoria 0002, South Africa

^d Department of Medical Research, China Medical University Hospital, China Medical University, Taichung, Taiwan

Received 29 November 2022; revised 2 January 2023; accepted 16 January 2023

Available online 24 February 2023

KEYWORDS

Appell hypergeometric;
Magneto hydrodynamics;
Porous medium;
Couple stress;
Nanofluid

Abstract The present paper investigates the magnetohydrodynamics Casson fluid flow with porous medium. The Cu-water nanofluid is used to investigate further analytical results. Thermal radiation is considered along with the Cattaneo-Christov heat flux model and then solved analytically, then expresses the closed forms analytical solution in terms of two variables of hypergeometric function. The special form of Appell hypergeometric solutions are closed form of analytical solutions. The results of normalized shear stress at the wall and temperature profile, and rate of heat flux can be analyzed with suitable parameters, Viz., relaxation time parameter, Prandtl number, Radiation parameter, Magnetic parameter, and so on. The newness of the current work's novelty is to explain a solution to issues with stretching sheets on the basis of Appell hypergeometric form and also investigation takes place on a time relaxation parameter. The shear stress $f_{\eta\eta}(0)$ is also calculated analytically. This problem has many industrial applications and engineering processes, namely glass-fiber production, extrusion of rubber sheets and so on. Finding that an increase in the thermal relaxation parameter and Prandtl number keeps the fluid temperature constant is the primary physical application.

© 2023 THE AUTHORS. Published by Elsevier BV on behalf of Faculty of Engineering, Alexandria University. This is an open access article under the CC BY-NC-ND license (<http://creativecommons.org/licenses/by-nc-nd/4.0/>).

1. Introduction

* Corresponding authors at: Department of Mechanical and Aeronautical Engineering, University of Pretoria, Pretoria 0002, South Africa (M. Sharifpur).

E-mail addresses: vishalaab99@gmail.com (A.B. Vishalakshi), u.s.m@davangereuniversity.ac.in (U.S. Mahabaleshwar), mhossein.ahmadi@shahroodut.ac.ir (M.H. Ahmadi), mohsen.sharifpur@up.ac.za (M. Sharifpur).

Peer review under responsibility of Faculty of Engineering, Alexandria University.

Due to the vast array of uses that non-Newtonian fluids have, they have received a lot of attention, namely, crude oil extraction from petroleum products, cooling of engines etc., (See Amin *et al.* [1]). Like this stretching sheet problems play a vital part in the engineering fields. Study of laminar flow problems first pioneered by Sakiadis [2] and later the work is extended by Crane [3], in this work the fluid flow happened because of stretching the sheet. Many researchers developed an examina-

Nomenclature

a	Positive constant	ν	Kinematic viscosity ($m^2 s^{-1}$)
B_0	Magnetic field strength (<i>Tesla</i>)	η	Similarity variable
C_P	Specific heat ($J K g^{-1} K^{-1}$)	θ	Dimensionless temperature field (K)
f	Transverse velocity	σ	Electrical conductivity (<i>siemens/meter</i>)
K	Permeability ($H m^{-1}$)	Λ	Casson fluid parameter
k	Thermal conductivity ($W m^{-1} K^{-1}$)	σ^*	Stefan-Boltzmann constant ($W m^{-2} K^{-4}$)
M	(= $\frac{\sigma_f B_0}{\rho_f a}$) Magnetic field parameter		
T	Temperature (K)		
<i>Greek Symbols</i>			
λ	Relaxation parameter	nf	Nanofluids
ρ	Density ($K g m^{-3}$)	f	Base fluid
μ	Dynamic viscosity ($K g m^{-1} s^{-1}$)	w	Quantities at wall
		∞	Quantities at freestream
		η	First order derivative

tion into the issues with stretching sheets as a result of their activities. Mahabaleshwar *et al.* [4–5], Tamayol *et al.* [6] worked on stretching sheet problems along with different mediums. Turkyilmazoglu [35] explained unsteady flow with MHD in the presence of deformable surfaces, here he uses the analytical method. See some other works of Turkyilmazoglu in the ref [36–37].

When a porous medium was present, fluid flow occurred. This phenomenon has many industrial applications. Later the stretching sheet problems are carried out with nanofluids along with different fluids and boundary conditions. Sharifpur *et al.* [7–9] worked on thermal characteristics of nanofluids and magnetorheological characteristics of some nanofluids are also reviewed. Mahabaleshwar *et al.* [10] and Benos *et al.* [11] studied on nanofluids with suction and laminar natural convection along with the computational time. Some other examples related to nanofluids are listed in [12–14]. The application of nanofluid is explained in the work of Ahmadi *et al.* [15]. Heat transmission and free convection flow were studied by Aman *et al.* [29] in the presence of CNTs Maxwell nanofluids with a range of molecular liquids. The MHD nanofluid flow on the surface of a thin film sprayed on a stretching cylinder with heat transfer was investigated by Khan *et al.* [30]. View further nanofluid examples in [31–33].

The above-mentioned works are only restricted to the momentum and energy equations with the classical Fourier law. Therefore, some investigation takes place on a time relaxation parameter, it is primarily studied by Cattaneo [16]. The ordinary type derivatives are converted into Oldroyd's upper convicted derivative, which, as improved by Christov [17], & it is recognized as heat flux of Cattaneo-Christov. Turkyilmazoglu [34] explained the heat transfer enhancement using Cattaneo-Christov heat flux model in the way of enhancing the heat transfer rate from the surfaces.

The preceding works served as inspiration for the current work, which describes the heat transfer properties of Casson fluid flow through a porous media with radiation. Casson fluid models usually describe the characteristics of non-Newtonian fluid behavior. The novelty of the current work is to describe the Casson fluid flow behaviour using analytical techniques, and nanoparticles are added to the fluid's surface to improve thermal efficiency. Also the main methodology explains that

the stretching sheet problem on the basis of analytical method by using Appell hypergeometric technique, with time relaxation parameter. In this ordinary type derivatives are converted into Oldroyd's upper convicted derivative by using the Cattaneo-Christov equation. then the temperature equation is solved by using direct integration. The main physical aspects of the present are in the field of industrial, biomedical and engineering processes. See the works of Mahabaleshwar *et al.* [18] and Anusha *et al.* [19] on Casson fluid flow.

2. Mathematical analysis

The current analysis analyses a non-Newtonian fluid flow in the presence of MHD and a porous media. Another fluid that is introduced into the flow is Cu-water nanofluid. Fig. 1. explains the schematic diagram used for this analysis. and Table 1 indicates the nanofluid amounts.

The Maxwell's equation

$$\begin{aligned}\vec{J} &= \mu_m \sigma (\vec{q} \times \vec{B}), \\ \nabla \cdot \vec{B} &= 0, \\ \nabla \times \vec{B} &= \sigma \vec{E}_{\text{ind}}, \\ \nabla \times \vec{E}_{\text{ind}} &= -\mu_m \frac{\partial \vec{B}}{\partial t},\end{aligned}\quad (a)$$

here $\vec{E}_{\text{ind}} = \mu_m \vec{q} \times \vec{B}$ stands for the induced electric field and others follow the nomenclature's definitions. In magneto-

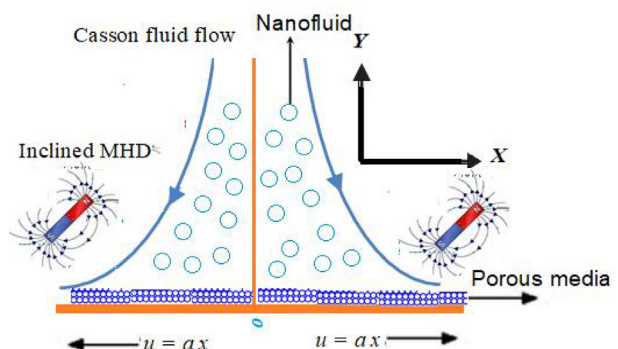


Fig. 1 Schematic diagram of Casson fluid flow.

Table 1 Quantities of base fluid and nanofluid.

Nano liquid physical properties	Liquid phase (water)	Copper	Alumina
$c_p(J/kgK)$	4179	385	765
$\rho(kg/m^3)$	997.1	8933	3970
$k(W/mK)$	0.613	400	40
$\sigma(Sm^{-1})$	0.05	5.97×10^7	

convection, the Maxwell equations are typically combined into a single equation known as the magnetic induction equation.

However, using the constitutive Eq. (1), the magnetic Rayleigh number $Rm = \mu_m \sigma Vd \ll 1$ (here V is Characteristic velocity) and the Lorentz force $\mu_m \vec{J} \times \vec{B}$ for weak conducting fluid can be written as.

$$\mu(\vec{J} \times \vec{B}) = -\mu^2 \sigma B_0^2 u$$

This is referred to as the magnetohydrodynamic problem's Hartmann formulation.

The altered N-S equations of the present problem listed as (See Siddheshwar *et al.* [23], Hussanan *et al.* [27], and Nadeem *et al.* [28]).

$$\frac{\partial u}{\partial x} + \frac{\partial v}{\partial y} = 0, \quad (1)$$

$$u \frac{\partial u}{\partial x} + v \frac{\partial v}{\partial y} = v_{nf} \left(1 + \frac{1}{\Lambda} \right) \frac{\partial^2 u}{\partial y^2} - \left(\frac{\sigma_{nf} B_0^2}{\rho_{nf}} \text{Sin}^2(\tau) + \frac{v_{nf}}{K} \right) u \quad (2)$$

$$(\rho c_P)_{nf} \left(u \frac{\partial T}{\partial x} + v \frac{\partial T}{\partial y} \right) = -(\nabla \vec{q} + q_r) \quad (3)$$

here, Λ indicates the Casson fluid parameter, K indicates permeability, q_r is the heat flux and \vec{q} is velocity vector.

The appropriate B.C s are

$$\left. \begin{array}{l} u = u_w = ax, \quad v = 0, \quad T = T_w, \quad \text{at } y = 0 \\ u \rightarrow 0, \quad T \rightarrow T_\infty \quad \text{as } y \rightarrow \infty \end{array} \right\} \quad (4)$$

here, u_w is the linear velocity, a is the positive constant, T_w and T_∞ are the wall and for field temperature.

The suitable similarity transformation:

$$u = ax f_\eta(\eta), \quad v = -\sqrt{av} f(\eta), \quad \theta(\eta) = \frac{T - T_\infty}{T_w - T_\infty}, \quad \eta = y \sqrt{\frac{a}{v}} \quad (5)$$

the terminology defines the variables that are used in the equations above.

3. Exact analysis of momentum equation:

Using Eq. (5), the momentum equation is transformed to

$$\begin{aligned} & \Gamma_2 f_{\eta\eta\eta} \left(1 + \frac{1}{\Lambda} \right) + \Gamma_1 \left(f_{\eta\eta} - f_\eta^2 \right) \\ & - (\Gamma_3 M \text{Sin}^2(\tau) + \Gamma_2 D a^{-1}) f_\eta \\ & = 0 \end{aligned} \quad (6)$$

The suitable boundary condition reduces to

$$f_\eta(0) = 1, \quad f'(0) = 0, \quad f_\eta(\infty) \rightarrow 0. \quad (7)$$

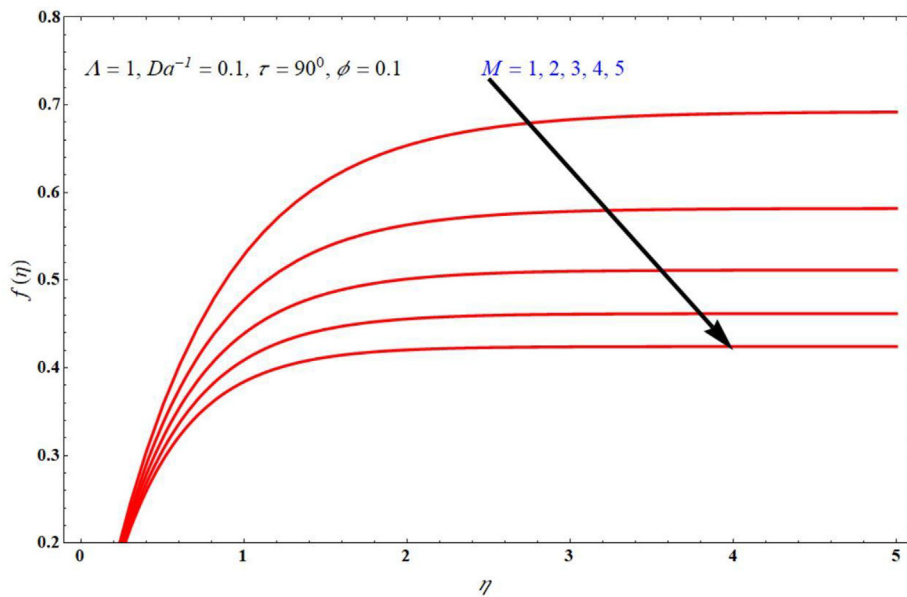


Fig. 2 The impact of $f(\eta)$ verses η for varying M values.

Assume the solution of Eq. (6) is of the form

$$f(\eta) = \frac{1}{\beta} (1 - \text{Exp}[-\beta\eta]), \quad (8)$$

By using this solution, the Eq. (6) can be reduced to

$$\beta = \sqrt{\frac{\Gamma_1 + \Gamma_3 M \sin^2(\tau) + \Gamma_2 D a^{-1}}{\Gamma_2 (1 + \frac{1}{\Lambda})}}. \quad (9)$$

4. Exact analysis of energy equation:

Cattaneo-Christov model gives the following equation,

$$q + \lambda \left(\frac{\partial q}{\partial t} + V \cdot \nabla q - q \nabla V + (\nabla \cdot V)q \right) = -k \nabla T. \quad (10)$$

By using Rosseland's approximation the term $\partial q_r / \partial y$ can be calculated (See Mahabaleshwar *et al.* [21–22]). Therefore, the Eq. (3) transformed into

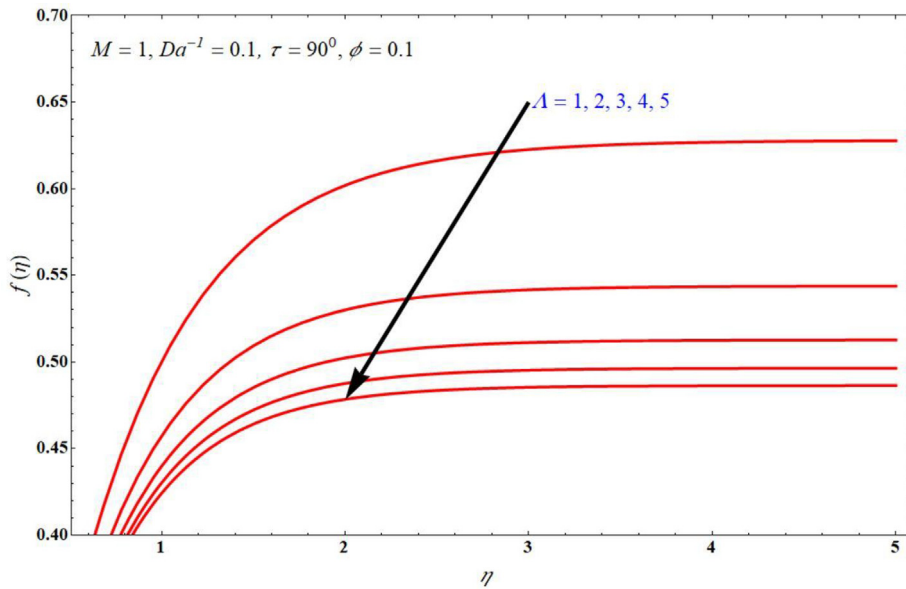


Fig. 3 $f(\eta)$ verses η for various Λ values.

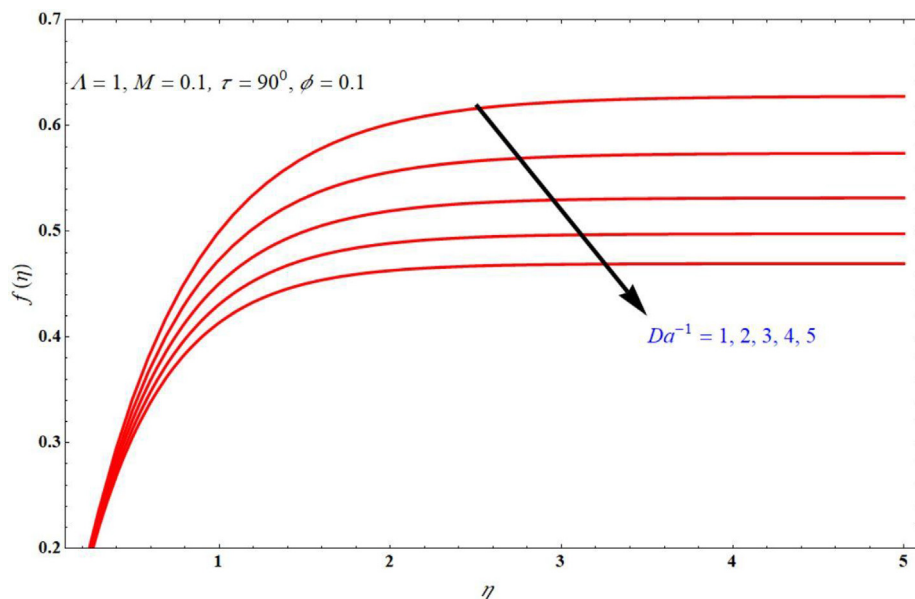


Fig. 4 Effect of $f(\eta)$ verses η for varying the $D a^{-1}$ values.

$$\begin{aligned} u \frac{\partial T}{\partial x} + v \frac{\partial T}{\partial y} + \lambda \left(u \frac{\partial u}{\partial x} \frac{\partial T}{\partial x} + v \frac{\partial v}{\partial y} \frac{\partial T}{\partial y} + u \frac{\partial u}{\partial x} \frac{\partial T}{\partial y} + v \frac{\partial v}{\partial y} \frac{\partial T}{\partial x} + 2uv \frac{\partial^2 T}{\partial x \partial y} + u^2 \frac{\partial^2 T}{\partial x^2} + v^2 \frac{\partial^2 T}{\partial y^2} \right) \\ = \frac{k_{nf}}{(\rho c_p)_{nf}} \frac{\partial^2 T}{\partial x^2} - \frac{1}{(\rho c_p)_{nf}} \frac{\partial q_r}{\partial y} \end{aligned} \quad (11)$$

On substitution of similarity variables defined in Eq. (5) into Eq. (11), then the solution of above equations is transformed into the following ordinary differential equation form.

$$\frac{1}{\Gamma_4} (\Gamma_5 + R) \theta_{\eta\eta} + \text{Pr} f \theta_\eta - \text{Pr} \gamma (f f_\eta \theta_\eta + f^2 \theta_{\eta\eta}) = 0 \quad (12)$$

where $Da^{-1} = \mu/\rho K a$ is inverse Darcy number, $M = \sigma_f B_0^2 / \rho_j a$ is Magnetic parameter, $Pr = k/\rho c_P$ is Prandtl number, $\gamma = a\lambda$ is the relaxation time parameter, $R = \frac{16\sigma T^3}{3k^* k}$ is the radiation parameter.

The boundary conditions of the energy equation reduced to,

$$\theta(0) = 1, \quad \theta(\infty) = 0$$

The nanofluid quantities used in the above results can be defined as (See Ahmadi *et al.* [24])

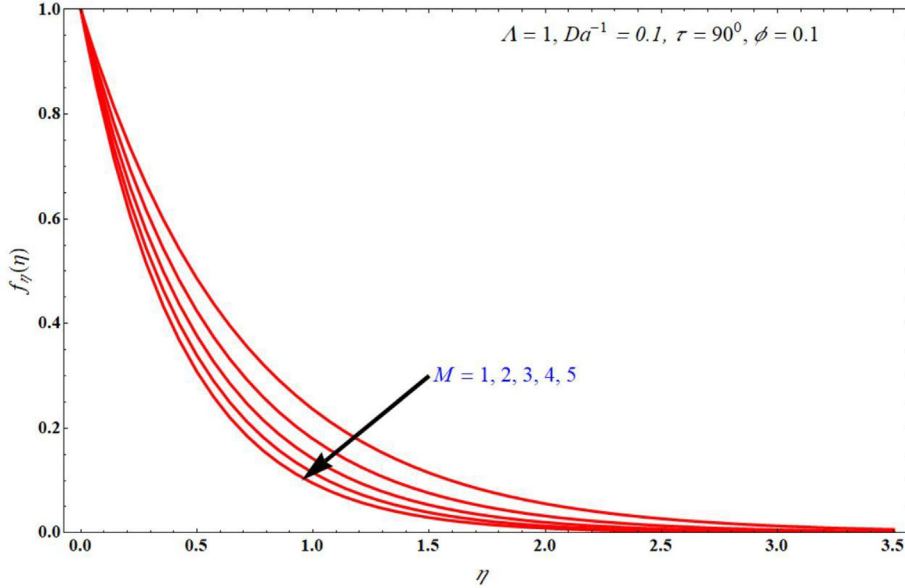


Fig. 5 The impact of $f_\eta(\eta)$ verses η for altering M values.

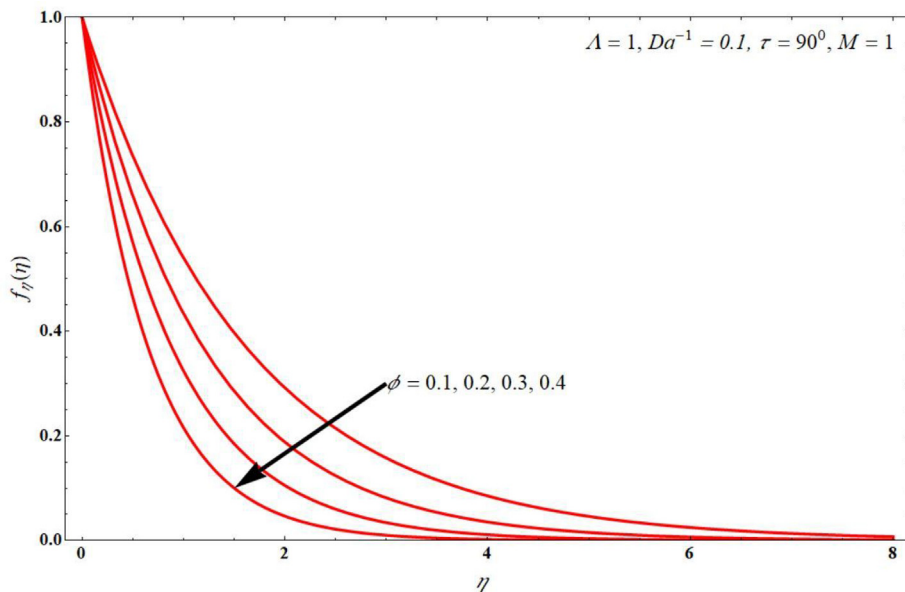


Fig. 6 $f_\eta(\eta)$ verses η for changing the values of ϕ .

$$\Gamma_1 = \frac{\rho_{nf}}{\rho_f}, \quad \Gamma_2 = \frac{\mu_{nf}}{\mu_f}, \quad \Gamma_3 = \frac{\sigma_{nf}}{\sigma_f}, \quad \Gamma_4 = \frac{(\rho c_p)_{nf}}{(\rho c_p)_f}, \quad \Gamma_5 = \frac{k_{nf}}{k_f}. \quad (14)$$

On rearranging Eq. (12) by using $f_\eta(\eta) = 1 - \beta f(\eta)$ into Eq. (12) to yield the result as

$$\theta_{\eta\eta} + \Gamma_4 \left(\frac{Pr\gamma\beta f^2 + (Pr - Pr\gamma)f}{(\Gamma_3 + R) - \Gamma_4\gamma Pr f^2} \right) \theta_\eta = 0 \quad (15)$$

Put $b(f) = \Gamma_4 \left(\frac{Pr\gamma\beta f^2 + (Pr - Pr\gamma)f}{(\Gamma_3 + R) - \Gamma_4\gamma Pr f^2} \right)$ for further calculation.

Eq. (15) can be rewritten as

$$\theta_{\eta\eta} + b(f)\theta_\eta = 0 \quad (16)$$

Eq. (16) can be solved into the following form

$$\theta(\eta) = 1 + \theta_\eta(0) \int_0^\eta e^{-\int_0^\eta b(f)d\eta} d\eta, \quad (17)$$

$$\theta_\eta(0) = -\frac{1}{\int_0^\infty e^{-\int_0^\eta b(f)d\eta} d\eta} \quad (18)$$

$$\begin{aligned} -\int_0^\eta b(f)d\eta &= -\int_0^{f(\eta)} \frac{b(f)}{(1-\beta f(\eta))} df(\eta), \\ &= \ln \left(\frac{(1-\beta f(\eta))^{-A}}{(1-sf(\eta))^{-B}(1+sf(\eta))^{-C}} \right). \end{aligned} \quad (19)$$

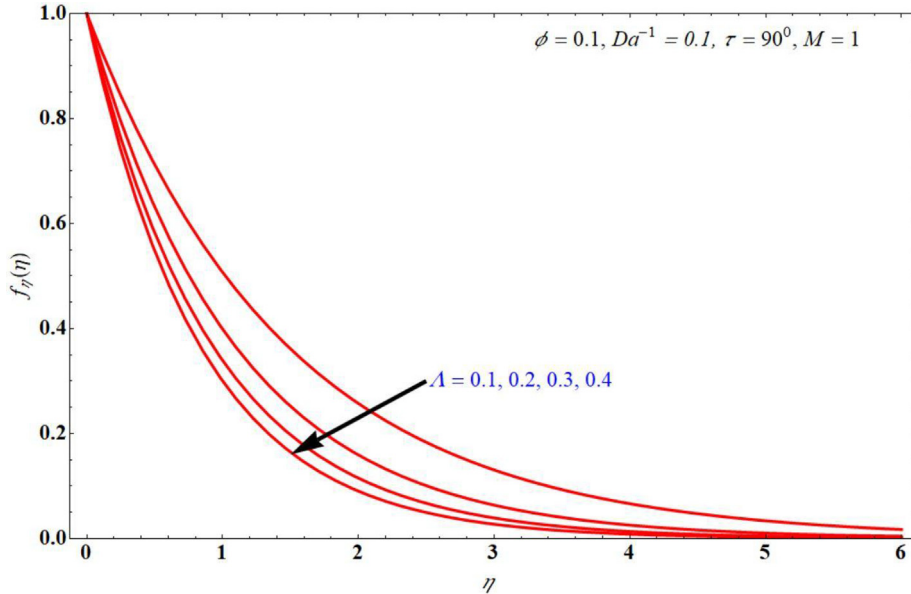


Fig. 7 $f_\eta(\eta)$ verses η for various M values.

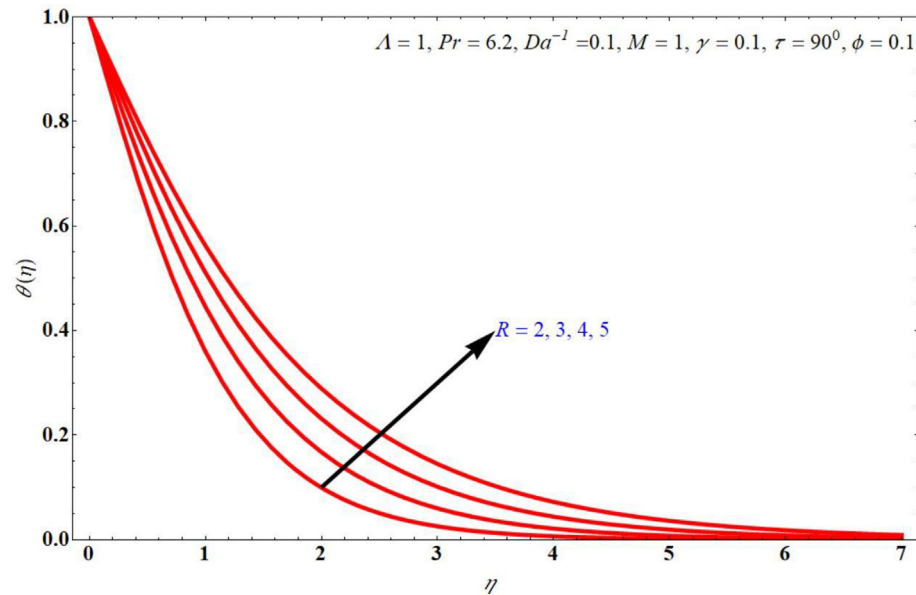


Fig. 8 $\theta(\eta)$ verses η for varying R values.

where,

$$\begin{aligned}
 A &= \left(\frac{\Gamma_4}{\Gamma_5+R}\right) \frac{Pr}{\frac{\gamma Pr \Gamma_4}{\Gamma_5+R} - \beta^2}, B = \frac{\beta \sqrt{\frac{Pr \Gamma_4}{\Gamma_5+R}} + \sqrt{\gamma} \left(\left(\frac{\Gamma_4}{\Gamma_5+R}\right) pr + \beta^2 - \gamma Pr \left(\frac{\Gamma_4}{\Gamma_5+R}\right) \right)}{2\sqrt{\gamma} \left(\left(\frac{\Gamma_4}{\Gamma_5+R}\right) - \beta^2 \right)}, \\
 c &= \frac{-\beta \sqrt{\frac{Pr \Gamma_4}{\Gamma_5+R}} + \sqrt{\gamma} \left(\left(\frac{\Gamma_4}{\Gamma_5+R}\right) pr + \beta^2 - \gamma Pr \left(\frac{\Gamma_4}{\Gamma_5+R}\right) \right)}{2\sqrt{\gamma} \left(\left(\frac{\Gamma_4}{\Gamma_5+R}\right) - \beta^2 \right)}, s \\
 &= \sqrt{\frac{\gamma Pr \Gamma_4}{\Gamma_5+R}}. \tag{20}
 \end{aligned}$$

Therefore, we write:

$$\int_0^\eta e^{-\int_0^\eta b(f)d\eta} d\eta = \int_0^{f(\eta)} \frac{(1 - \beta f(\eta))^{-A-1}}{(1 - sf(\eta))^{-B}(1 + sf(\eta))^{-C}} df(\eta). \tag{21}$$

Eq. (21) is solved in terms of Appell hypergeometric function and it is given by

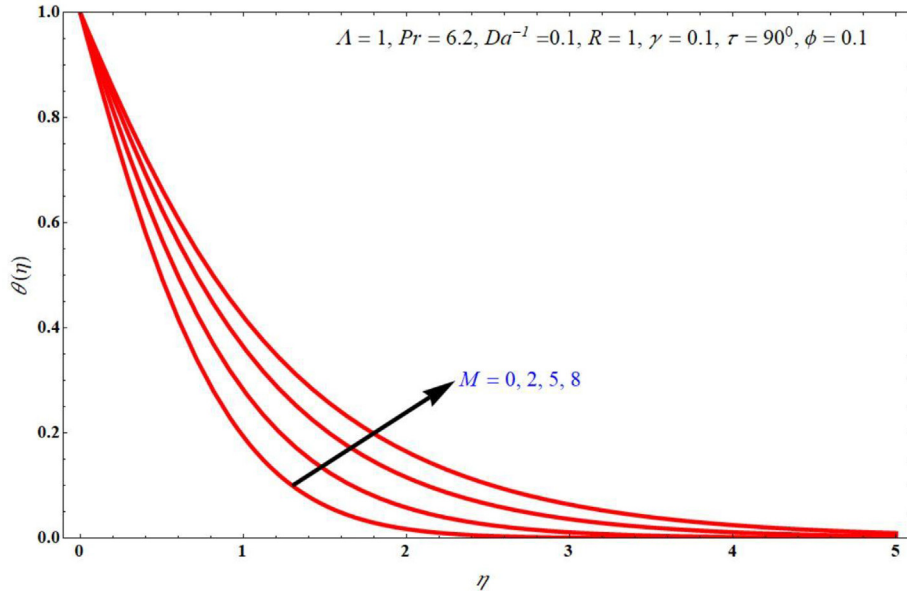


Fig. 9 $\theta(\eta)$ verses η for changing M values.

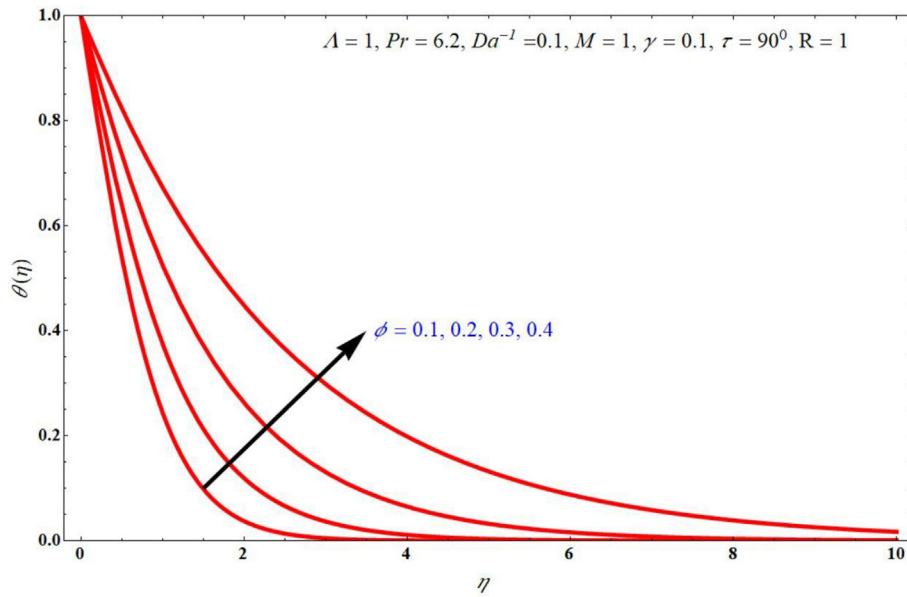


Fig. 10 The plots of $\theta(\eta)$ verses η for changing the values of ϕ .

$$\int_0^{f(\eta)} \frac{(1-\beta f(\eta))^{-A-1}}{(1-sf(\eta))^{-B}(1+sf(\eta))^{-C}} df(\eta) = \frac{1}{A\beta} (1-\beta f(\eta))^{-A} (1-sf(\eta))^B (1+sf(\eta))^C \left(\frac{\beta-\beta sf(\eta)}{\beta-s} \right)^{-B} \left(\frac{\beta+\beta sf(\eta)}{\beta+s} \right)^{-C} F_1 \left(-A; -B, -C; -A+1, \frac{s(\beta f(\eta)-1)}{\beta-s}, \frac{-s(\beta f(\eta)-1)}{\beta+s} \right) \Big|_0^{f(\eta)}. \quad (22)$$

On substituting the following property into Eq. (20)

$$F_1(\alpha; \beta, \beta'; \beta + \beta'; x, y) = (1-y)_2^{\alpha} F_1(\alpha, \beta; \beta + \beta', \frac{x-y}{1-y}). \quad (23)$$

Therefore, the result yields as

$$\int_0^{f(\eta)} \frac{(1-\beta f(\eta))^{-A-1}}{(1-sf(\eta))^{-B}(1+sf(\eta))^{-C}} df(\eta) = \frac{1}{A\beta} (1-\beta f(\eta))^{-A} (1-sf(\eta))^B (1+sf(\eta))^C \left(\frac{\beta-\beta sf(\eta)}{\beta-s} \right)^{-B} \left(\frac{\beta+\beta sf(\eta)}{\beta+s} \right)^{-C} F_1 \left(-A; -B, -C; -A+1, \frac{s(\beta f(\eta)-1)}{\beta-s}, \frac{-s(\beta f(\eta)-1)}{\beta+s} \right) \Big|_0^{f(\eta)}. \quad (24)$$

On substituting integration bond $0 \rightarrow \frac{1}{\beta}$ to get the finite result

$$\lim_{\eta \rightarrow 0; f(\eta) \rightarrow 0} \left(\int e^{- \int_0^\eta b(f) d\eta} d\eta \right) = \frac{\left(\frac{\beta-s}{\beta} \right)^B \left(\frac{\beta-s}{\beta} \right)^{C-A}}{A\beta} {}_2 F_1 \left(-A, -B; -B-C; \frac{-2s}{(\beta-s)} \right) \quad (25)$$

On considering $f(\eta) \rightarrow \frac{1}{\beta}$, then it is check that

$$\lim_{\eta \rightarrow 0; f(\eta) \rightarrow 0} \left(\int_0^\infty e^{- \int_0^\eta b(f) d\eta} d\eta \right) = \begin{cases} \rightarrow \infty & A > 0 \\ \rightarrow 0 & A < 0 \end{cases} \quad (26)$$

From Eq.(26) it is easy to conclude that $A < 0$ is the only reasonable case.

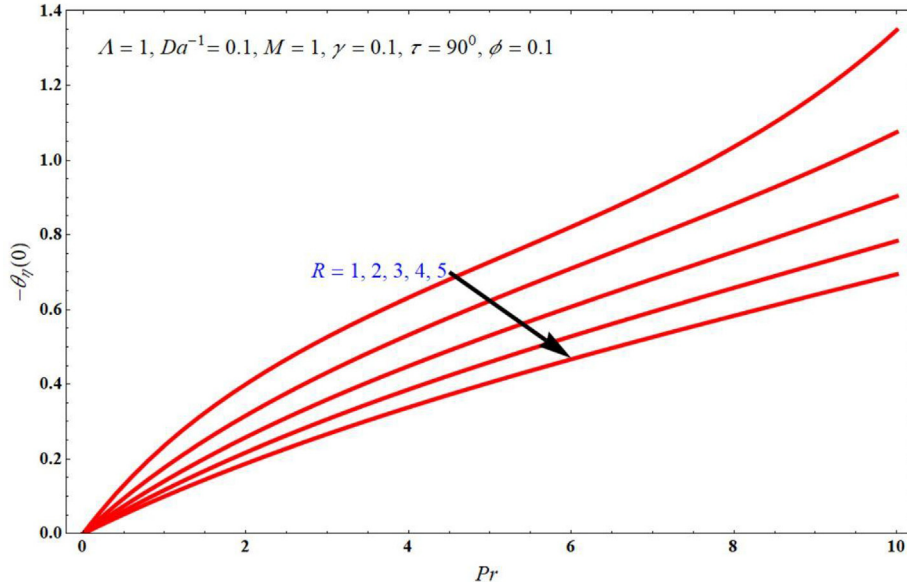


Fig. 11 Plots of $-\theta_\eta(0)$ verses Pr for changing the values of R .

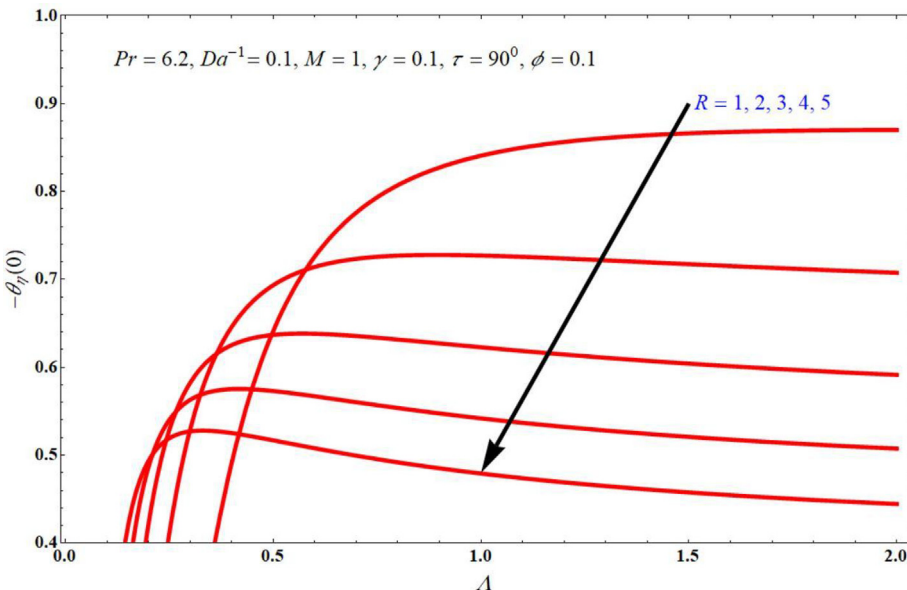


Fig. 12 Plots of $-\theta_\eta(0)$ verses Λ for altering the values of R .

$$\text{If, } \gamma \Pr \left(\frac{\Gamma_4}{\Gamma_5 + R} \right) < f_{\eta\eta}(0)^2 \quad (27)$$

By using Eq. (9)

$$\gamma \left(1 + \frac{1}{\Lambda} \right) < \left(\frac{(\Gamma_5 + R)(\Gamma_1 + \Gamma_3 M \sin(\tau)^2 + \Gamma_2 Da^{-1})}{\Pr \Gamma_2 \Gamma_4} \right) \quad (28)$$

For incompressible 2D flow the results for for (6) and (12) can be examined as

$$f(\eta) = \frac{1}{\beta} (1 - \text{Exp}[-\beta\eta]), \quad (29)$$

On using Eq.(29) we can get the value of $f_{\eta\eta}(0)$ is

$$f_{\eta\eta}(0) = -\beta = -\sqrt{\frac{\Gamma_1 + \Gamma_3 M \sin^2(\tau) + \Gamma_2 Da^{-1}}{\Gamma_2 (1 + \frac{1}{\Lambda})}} \quad (30)$$

If the condition $f_{\eta\eta}(0)^2 > \gamma \Pr$

$$\theta_\eta(0) = \frac{A \beta \left(\frac{\beta}{\beta-s} \right)^B \left(\frac{\beta}{\beta+s} \right)^{C-A}}{{}_2F_1(-A, -B; -B-C; \frac{-2s}{(\beta-s)})} \quad (31)$$

$$\theta(\eta) = \left(\frac{1 + \frac{s}{\beta} (1 - e^{-\beta\eta})}{e^{-\beta\eta}} \right) \frac{{}_2F_1(-A, -B; -B-C; \frac{-2s\beta e^{-\beta\eta}}{(\beta+s)(\beta-s)})}{{}_2F_1(-A, -B; -B-C; \frac{-2s}{(\beta-s)})} \quad (32)$$

where,

$$A = \left(\frac{\Gamma_4}{\Gamma_5 + R} \right) \frac{\Pr}{\frac{\Pr \Gamma_4}{\Gamma_5 + R} - \beta^2}, B = \frac{\beta \sqrt{\frac{\Pr \Gamma_4}{\Gamma_5 + R}} + \sqrt{\gamma} \left(\left(\frac{\Gamma_4}{\Gamma_5 + R} \right) \Pr + \beta^2 - \gamma \Pr \left(\frac{\Gamma_4}{\Gamma_5 + R} \right) \right)}{2\sqrt{\gamma} \left(\left(\frac{\Gamma_4}{\Gamma_5 + R} \right) - \beta^2 \right)}, \\ C = \frac{-\beta \sqrt{\frac{\Pr \Gamma_4}{\Gamma_5 + R}} + \sqrt{\gamma} \left(\left(\frac{\Gamma_4}{\Gamma_5 + R} \right) \Pr + \beta^2 - \gamma \Pr \left(\frac{\Gamma_4}{\Gamma_5 + R} \right) \right)}{2\sqrt{\gamma} \left(\left(\frac{\Gamma_4}{\Gamma_5 + R} \right) - \beta^2 \right)}, S = \sqrt{\frac{\gamma \Pr \Gamma_4}{\Gamma_5 + R}}$$

It is directly obtain the classic solutions by equating $\gamma \rightarrow 0$.

5. Results and discussion

An incompressible Casson fluid flow with MHD & containing a medium of porous is analyzed in the present analysis. Cu-Water nanofluid is taken into further investigation. Then the obtained resulting equations are solved in the form of Appell hypergeometric equation. Using Radiation parameter, magnetic parameter, and solid volume fraction etc., the results can be checked. The range of physical parameters used in the present problem is that the value of $\Pr = 6.2, \phi = 0.1, \Lambda = 0$ to ∞ , all other parameters varied with suitable value to get suitable parameters. The current study is based on Cattaneo-Christovs theory which took into account the importance of downtime. These temperature-dependent variations in thermal conductivity properties.

Fig. 2 indicates that the effect of $f(\eta)$ verses η for different M values. In this, $f(\eta)$ values drop with raises M values. A similar effect is observed in Fig. 3 when we vary the Λ values, i.e. on raising the values of Λ the $f(\eta)$ decreases. The impact of $f(\eta)$ on η for taking the values of Da^{-1} in increasing order is

observed at Fig. 4. It is seen that the $f(\eta)$ is decreases for more value of Da^{-1} , and it has more value at small values of Da^{-1} .

Fig. 5 and Fig. 6 illustrated the effect of $f_\eta(\eta)$ verses η for different M values, and ϕ respectively. In Fig. 5, $f_\eta(\eta)$ is inversely proportional to the values of M . This same impact is seen in Fig. 6, here $f_\eta(\eta)$ decays on raising the values of ϕ . The impact of $f_\eta(\eta)$ verses η for the values of Λ is taken in increasing order represented in Fig. 7. In this, $f_\eta(\eta)$ is inversely proportional to Λ , i.e. $f_\eta(\eta)$ is more for smaller values of Λ .

Figs. 8 & 9 portrays the impact of $\theta(\eta)$ verses η for varying the values of R and M respectively. In Fig. 8, we conclude that the $\theta(\eta)$ raises with raising the values of R . similarly $\theta(\eta)$ increases with increases of M , it is indicated in Fig. 9.

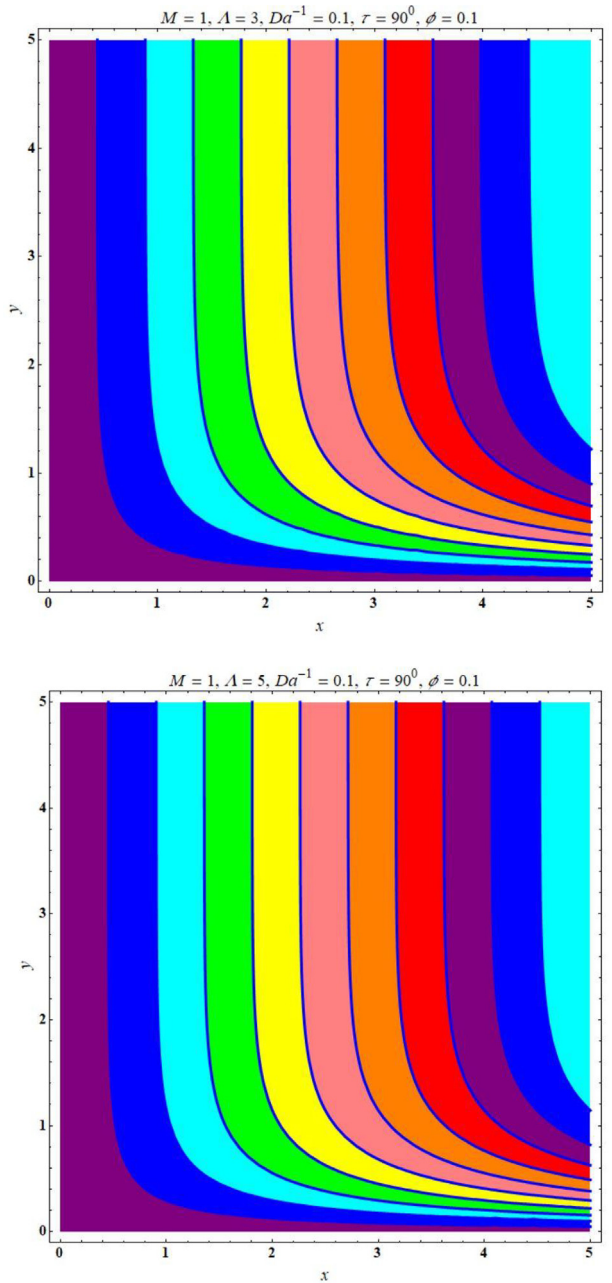


Fig. 13 (a,b): Streamline graphs for $\Lambda = 3$, & $\Lambda = 5$.

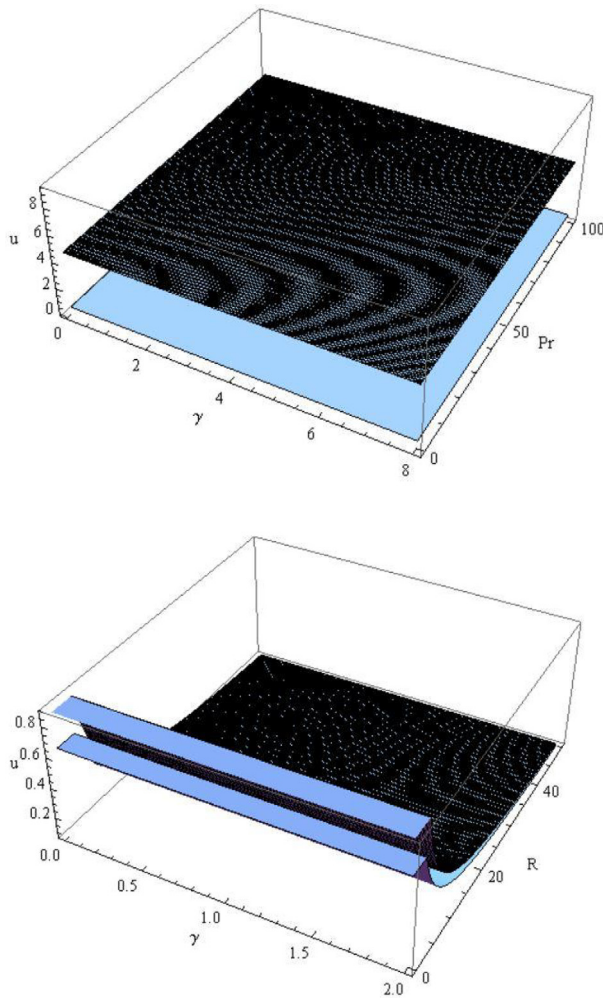


Fig. 14 (a,b):3-D graphs for the functions of γ & Pr , γ & R

Fig. 10 indicates $\theta(\eta)$ verses η for various values of ϕ , in this $\theta(\eta)$ increases with increasing the values of ϕ .

Figs. 11 & 12 represents the plots of $-\theta_\eta(0)$ for varying R values as a function of Pr and Λ respectively. In this, it could clearly conclude that $-\theta_\eta(0)$ is inversely proportional to R and Pr . **Fig. 13(a,b)** indicates the graphs with streamline for different values Λ . Also, **Fig. 14(a,b)** illustrate the 3-D graphs for the functions of γ & Pr , γ & R respectively.

6. Conclusion:

The present research examines the flow of a non-Newtonian and incompressible fluid in the presence of MHD, a porous medium with an inverse Darcy number, and heat radiation. The resulting equations are analytically solved, and the Appell hypergeometric equation is used to express the outcome. Cu-water nanofluid is also employed to analyse the outcome. We arrive to the following conclusions by utilising this solution.

- Transverse and tangential velocities decrease by adding M
- $f(\eta)$ increases with increasing the values of Λ

- ϕ is inversely proportional to $f_\eta(\eta)$
- Present paper is well argument with Amin *et al.* [20].
- The work of Crane is recovered from Eq. (9) if $M = Da^{-1} = 0$, $\Gamma_1 = \Gamma_2 = \Gamma_3 = 1$, $\Lambda \rightarrow \infty$, and, $\tau = 90^\circ$.
- Mahabaleshwar *et al.* [25] is recovered from Eq. (9) if $M = 1$, $Da^{-1} = 0$, $\Gamma_1 = \Gamma_2 = \Gamma_3 = 1$, $\Lambda \rightarrow \infty$, and, $\tau = 90^\circ$, including Walter's liquid B term.
- Mahabaleshwar *et al.* [26] is recovered if $M = 1$, $Da^{-1} = 0$, $\Gamma_1 = \Gamma_2 = \Gamma_3 \neq 0$, and, $\Lambda \rightarrow \infty$, including Walter's liquid B term.
- Amin *et al.* [20] is recovered if $M = 1$, $Da^{-1} = 0$, $\Gamma_1 = \Gamma_2 = \Gamma_3 = 0$, $\Lambda \rightarrow \infty$, including Walter's liquid B term.

Declaration of Competing Interest

The authors declare that they have no known competing financial interests or personal relationships that could have appeared to influence the work reported in this paper.

References

- [1] M.M. Amin, M.H. Ahmadi, M.B. Fatemeh Joda, V. Antonio, S. Uson, Exergy analysis of a Combined Cooling Heating and power system integrated with wind turbine and compressed air energy storage system, Eng. Conv. Management. 131 (2017) 69–78.
- [2] B.C. Sakiadis, Boundary layer behaviour on continuous solid surface, AIChE J. 7 (1961) 26.
- [3] L.J. Crane, Flow past a stretching plate, Zeitschrift fur Angewandte Mathematik und Physik 21 (1970) 645–647.
- [4] U.S. Mahabaleshwar, I.E. Sarris, A.H. Antony, G. Lorenzini, I. Pop, An MHD couple stress fluid due to a perforated sheet undergoing linear stretching with heat transfer, Int. Jour. Heat Mass Transf. 105 (2017) 157–167.
- [5] U.S. Mahabaleshwar, K.R. Nagaraju, P.N. Vinay Kumar, D. Baleanu, G. Lorenzini, An exact analytical solution of the unsteady magnetohydrodynamics nonlinear dynamics of laminar boundary layer due to an impulsively linear stretching sheet, Continuum mech. Therm. 29 (2017) 559–567.
- [6] A. Tamayol, K. Hooman, M. Bahrami, Thermal analysis of Flow in a porous medium over a permeable stretching wall, Transp Porous med 85 (2010) 661–676.
- [7] M. Sharifpur, A.A. Saheed, J.P. Mayer, Experimental investigation and model development for effective viscosity of Al_2O_3 -glycerol nanofluids by using dimensional analysis and GMDH-NN methods, Int. Commun. Heat Mass Transf. 68 (2015) 208–219.
- [8] M. Sharifpur, S. yousefi, J.P. Meyer. A new model for density of nanofluids including nanolayer. Int. Commun. Heat Mass Transf. 78, (2016), 168–174.
- [9] M. Sharifpur, N. Tshimanga, J.P. Mayer, O. Manca, Experimental investigation and model development for thermal conductivity alpha- Al_2O_3 -glycerol nanofluids, Int. Commun. Heat Mass Transf. 85 (2017) 12–22.
- [10] U.S. Mahabaleshwar, P.N. Vinay Kumar, M. Sheremet, Magnetohydrodynamics flow of a nanofluid driven by a stretching/shrinking sheet with suction, Springer plus. 5 (2016) 1–9.
- [11] L.T. Benos, N.D. Polychronopoulos, U.S. Mahabaleshwar, G. Lorenzini, I.E. Sarris, Thermal and flow investigation of MHD natural convection in a nanofluid saturated porous

- enclosure: an asymptotic analysis, *J. Therm. Anal. Calorim.* 1–15 (2019).
- [12] M. Sharifpur, A.B. Solomon, T.L. Ottermann, J.P. Mayer, Optimum concentration of nanofluids for heat transfer enhancement under cavity flow natural convection with TiO_2 -water, *Int. Commun. Heat and Mass Transf.* 98 (2018) 297–303.
- [13] M. Sharifpur, N. Tshimanga, J.P. Mayer. Parametric analysis of effective thermal conductivity models for nanofluids. *ASME Int. Jour. Mech. Eng. Congress and Exposition.* 45257, (2012), 1-11.
- [14] M. Sharifpur, O.G. Solomon, K.Y. Lee, H. Ghodsinezhad, J.P. Mayer, Experimental investigation into natural convection of Zinc Oxide/water nanofluids in a square cavity, *Heat Transf. Eng.* (2020) 1–13.
- [15] M.H. Ahmadi, M.A. Nazari, R. Ghasempour, H. Madah, M.B. Shafii, M.A. Ahmadi. Thermal conductivity ratio prediction of Al_2O_3 /water nanofluid by applying connectionist methods. *Collides and Surfaces A: Physicochemical and Eng. Aspects.* 541, 154-164.
- [16] C. Cattaneo, Sulla conduzione del calore, *Atti Semin, Mat. Fis. Univ. Modena Reggio Emilia.* 3 (1948) 83–101.
- [17] C.I. Christov, On frame indifferent formulation of the Maxwell-Cattaneo model of finite-speed heat conduction, *Mech. Res. Commun.* 36 (2009) 481–486.
- [18] U.S. Mahabaleshwar, M.B. Rekha, P.N. Vinay Kumar, F. Selimefendigil, P.H. Sakanaa, G. Lorenzini, S.N. Ravichandra Nayakar, Mass transfer characteristics of MHD Casson fluid flow past stretching/shrinking sheet, *Jour. Eng. Therm. Phys.* 29 (2020) 285–302.
- [19] T. Anusha, Huang-Nan Huang, U.S. Mahabaleshwar. Two dimensional unsteady stagnation point flow of Casson hybrid nanofluid over a permeable flat surface and heat transfer analysis with radiation. *Jour. Taiwan Inst. Chem. Eng.* (2021).
- [20] J. Amin, M. Turkyilmazoglu, I. Pop, Threshold for the generalized Non-Fourier heat flux model: Universal closed form analytical solution, *Int. Commun. Heat and Mass Transf.* 123 (2021) 105204.
- [21] U.S. Mahabaleshwar, T. Anusha, P.H. Sakanaa, S. Bhattacharyya, Impact of Lorentz force and Schmidt number on chemically reactive Newtonian fluid flow on a stretchable surface when Stefan blowing and thermal radiation and significant, *Arabian Jour. Sci. Eng.* (2021) 1–17.
- [22] U.S. Mahabaleshwar, K.N. Sneha, Huang-Nan-Huang. An effect of MHD and radiation on CNTS-water based nanofluid due to a stretching sheet in a Newtonian fluid. Case studies of thermal engineering. (2021).
- [23] P.G. Siddheshwar, A. Chan, U.S. Mahabaleshwar. Suction-induced magneto hydrodynamics of a viscoelastic fluid over a stretching surface within a porous medium. *The IMA, J Appl. Mathematics.* 79, (2014), 445-458.
- [24] M.H. Ahmadi et, M. Amin, M.A. Nazari, R. Ghasempour. A review of thermal conductivity of various nanofluids. *Jour. Mol. Liq.* 265, 181-188.
- [25] U.S. Mahabaleshwar, I.E. Sarris, G. Lorenzini, Effect of radiation and Navier slip boundary of Walters' liquid B flow over a stretching sheet in a porous media, *Int. J. Heat Mass Transf.* 127 (2018) 1327–1337.
- [26] U.S. Mahabaleshwar, K.N. Sneha, M. Hatami, Effect of Cattaneo-Christov approximation for viscoelastic fluid with carbon nanotubes on flow and heat transfer, *Sci. Rep.* 12 (2022) 9485.
- [27] H. Abid, Z. Ismail, I. Khan, G.H. Atheer, S. Shafie, Unsteady boundary layer MHD free convection flow in a porous medium with constant mass diffusion and Newtonian heating, *The Eur. Jour. Plus.* 129 (2014) 46.
- [28] A.S. Nadeem, D.L.C. Ching, I. Khan, D. Kumar, K.S. Nisar, A new model of fractional Casson fluid based on generalized Fick's and Fourier's laws together with heat and mass transfer, *Alex. Eng. J.* 59 (2020) 2865–2876.
- [29] S. Aman, I. Khan, Z. Ismail, M.Z. Salleh, Q.M. Al-Mdallal, Heat transfer enhancement in free convection flow of CNTs Maxwell nanofluids with four different types of molecular liquids, *Sci. Rep.* 7 (2017) 2445.
- [30] N.S. Khan, T. Gul, S. Islam, I. Khan, A.M. Alqahtani, A.S. Alshomrani, Magnetohydrodynamic Nanoliquid Thin Film Sprayed on a Stretching Cylinder with Heat Transfer, *Appl. Sci.* 7 (2017) 271.
- [31] M. Sheikholeslami, Z. Shah, A. Shafee, I. Khan, I. Thilli, Uniform magnetic force impact on water based nanofluid thermal behavior in a porous enclosure with ellipse shaped obstacle, *Sci. Rep.* 9 (2019) 1196.
- [32] G. Aaiza, I. Khan, S. Shafie, Energy Transfer in Mixed Convection MHD Flow of Nanofluid Containing Different Shapes of Nanoparticles in a Channel Filled with Saturated Porous Medium, *Nanoscale Res Lett* 10 (2015) 490.
- [33] U. Khan, A. Zaib, I. Khan, K.S. Nisar. Activation energy on MHD flow of titanium alloy (Ti6Al4V) nanoparticle along with a cross flow and stream-wise direction with binary chemical reaction and non-linear radiation, *J. Mater. Res. Technol.* 9 (1), 188–19.
- [34] M. Turkyilmazoglu, Heat Transfer Enhancement Feature of the Non-Fourier Cattaneo-Christov Heat Flux Model, *J. Heat Transfer.* 143 (2021) 094501.
- [35] M. Turkyilmazoglu, K. Naganthran, I. Pop, Unsteady MHD rear stagnation-point flow over off-centred deformable surfaces, *Int. J. Num. Meth. Heat and Fluid flow.* 27 (2017) 1554–1570.
- [36] M. Turkyilmazoglu, Flow and heat over a rotating disk subject to a uniform horizontal magnetic field, *Zeitschrift für Naturforschung A* (2022) 2021–10350.
- [37] M. Turkyilmazoglu, Slip flow and heat transfer over a specific wedge: an exactly solvable Falkner-Skan equation, *J. Eng. Math.* 92 (2015) 73–81.